RSC Advances

PAPER

View Article Online
View Journal | View Issue

Cite this: *RSC Adv.*, 2017, **7**, 22735

Myrtucomvalones A–C, three unusual triketone–sesquiterpene adducts from the leaves of *Myrtus communis* 'Variegata'†

Ming Chen,‡[ab] Li-Feng Chen,‡[b] Man-Mei Li,[bc] Ni-Ping Li,[b] Jia-Qing Cao,[b] Ying Wang,[bc] Yao-Lan Li,[bc] Lei Wang*[bc] and Wen-Cai Ye *[abc]

Received 23rd February 2017
Accepted 17th April 2017

DOI: 10.1039/c7ra02260c

rsc.li/rsc-advances

Three new triketone–sesquiterpene adducts, myrtucomvalones A–C (**1–3**), along with four known compounds (**4–7**) were isolated from the leaves of *Myrtus communis* 'Variegata'. Compounds **1** and **2** are the first examples of triketone–cubebane hybrids with an unusual carbon skeleton. Their structures with absolute configurations were determined by spectroscopic data, single crystal X-ray diffraction and electronic circular dichroism (ECD) analyses. Compounds **1–7** displayed inhibitory activities against respiratory syncytial virus (RSV).

Introduction

Triketone–terpene adducts are widely present in the family Myrtaceae as important secondary metabolites, which have diverse carbon skeletons and possess antimicrobial, antitumor, and anti-inflammatory activities.[1–5] The plant *Myrtus communis* 'Variegata' (Myrtaceae), a colored-leafed evergreen shrub, is native to the Mediterranean region and has been traditionally used as a disinfectant and antiseptic agent.[6] Previous phytochemical investigations on some plants of the genus Myrtus had led to the isolation of terpenoids, flavonoids, and meroterpenoid derivatives including triketone–terpene adducts.[7–11] However, the chemical constituents of *Myrtus communis* 'Variegata' have not been reported. As part of our search for structurally unique and biologically active constituents from Myrtaceae plants,[11–16] three new sesquiterpene-based meroterpenoids, myrtucomvalones A–C (**1–3**), together with four known analogs (**4–7**) were isolated from the leaves of the title plant (Fig. 1). Compounds **1** and **2** represent the first examples of cubebane-based triketone–terpene adducts with an unusual skeleton. The structures and absolute configurations of these new compounds were elucidated by spectroscopic analysis, X-ray diffraction, and electronic circular dichroism (ECD) calculations. Moreover, compounds **1–7** exhibited inhibitory activities against respiratory syncytial virus (RSV) with IC_{50} values ranging from 11.67 ± 0.95 to 46.33 ± 3.75 μM. In this paper, we describe the isolation, structural elucidation, and anti-RSV activities of **1–7**.

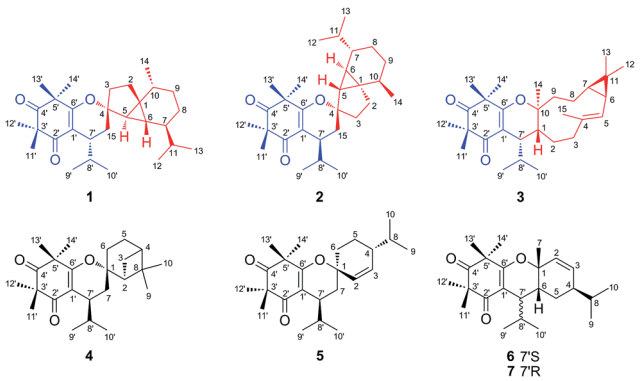

Fig. 1 Chemical structures of **1–7**.

Results and discussion

Compound **1** was obtained as colorless blocks. The HR-ESI-MS of **1** showed a quasimolecular ion peak at *m/z* 441.3369 $[M + H]^+$ (calcd for $C_{29}H_{45}O_3$, 441.3363), consistent with the molecular formula $C_{29}H_{44}O_3$ with 8 degrees of unsaturation. The UV spectrum of **1** displayed absorption maximum at 268 nm. The IR spectrum revealed characteristic absorptions for conjugated carbonyl (1651 cm^{-1}) and olefinic bond (1620 cm^{-1}). The ^1H NMR spectrum of **1** suggested the presence of four tertiary

[a]*Department of Natural Medicinal Chemistry, China Pharmaceutical University, Nanjing 210009, P. R. China. E-mail: chywc@aliyun.com; Tel: +86-20-85221559*
[b]*Institute of Traditional Chinese Medicine & Natural Products, JNU-HKUST Joint Laboratory for Neuroscience & Innovative Drug Research, College of Pharmacy, Jinan University, Guangzhou 510632, P. R. China. E-mail: cpuwanglei@126.com*
[c]*Guangdong Province Key Laboratory of Pharmacodynamic Constituents of TCM and New Drugs Research, Jinan University, Guangzhou 510632, P. R. China*

† Electronic supplementary information (ESI) available: UV, IR, NMR and HR-ESI-MS spectra of compounds **1–3**. Single-crystal X-ray data of **1** and **2**. Quantum chemical CD calculation of compounds **2** and **3**. CCDC 1529330 and 1529333. For ESI and crystallographic data in CIF or other electronic format see DOI: 10.1039/c7ra02260c

‡ These authors have contributed equally to this work.

methyls [δ_H 1.29 (3H, s, H-11′), 1.40 (3H, s, H-12′), 1.32 (3H, s, H-13′), and 1.32 (3H, s, H-14′)], a secondary methyl [δ_H 1.04 (3H, d, J = 6.5 Hz, H-14)], and two isopropyl moieties [δ_H 2.56 (1H, m, H-8′), 0.68 (3H, d, J = 6.5 Hz, H-9′), 0.93 (3H, d, J = 6.5 Hz, H-10′), 1.59 (1H, overlapped, H-11), 0.95 (3H, d, J = 5.5 Hz, H-12), and 0.91 (3H, d, J = 5.5 Hz, H-13)]. The ^{13}C NMR and DEPT spectra of **1** exhibited 29 carbon signals including those for an olefinic bond, two carbonyls and 25 aliphatic carbons. With the aid of ^{1}H–^{1}H COSY, HSQC, HMBC, and NOESY experiments, the NMR signals of **1** could be assigned as shown in Table 1. A comparison of the NMR data of **1** with those of the known compounds viminadiones A and B[17] suggested the presence of an isobutyl syncarpic acid unit (a) (Fig. 1). The remaining 15 aliphatic carbon atoms could be attributable to a sesquiterpene moiety.[11,18] The ^{1}H–^{1}H COSY spectrum of **1** demonstrated the presence of three spin systems (H-15 to H-9′/H-10′, H-2 to H-3 and H-5 to H-14) (Fig. 2). In addition, the HMBC correlations between Me-14 and C-1/C-9, between H_2-3 and C-1/C-4/C-5, between H_2-2 and C-1, and between H-15 and C-4 suggested the presence of a cubebane moiety (b) in **1** (Fig. 2). Furthermore, the HMBC cross-peaks between H-7′ and C-1′, and between H-15 and C-1′ indicated the connection of the cubebane and trikentone units *via* a C-7′ and C-15 bond. Based on the molecular

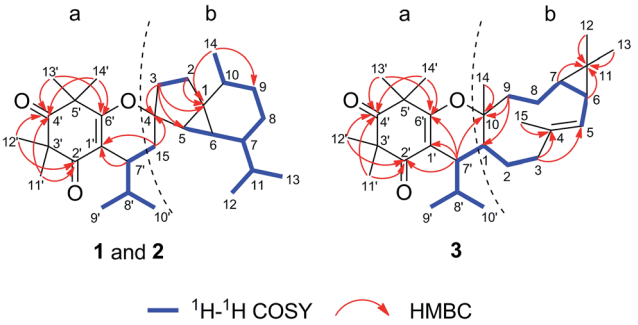

Fig. 2 Key ^{1}H–^{1}H COSY and HMBC correlations of **1–3**.

Table 1 ^{1}H and ^{13}C NMR data of **1–3**

	1[a]		**2**[a]		**3**[a]	
No.	δ_H[b] (J in Hz)	δ_C	δ_H[b] (J in Hz)	δ_C	δ_H[b] (J in Hz)	δ_C
1	—	34.7	—	33.3	1.92 m	37.4
2	α 2.01 ddd (12.5, 11.5, 8.5) β 1.51 dd (12.5, 8.5)	29.7	α 1.58 β 1.89 ddd (12.5, 11.5, 8.5)	29.4	1.45	33.4
3	α 1.60 β 1.14 ddd (14.5, 11.5, 8.5)	31.8	α 1.13 ddd (12.5, 11.5, 8.5) β 1.75	30.3	2.15	40.7
4	—	90.5	—	88.9	—	136.8
5	1.05	37.0	0.95	37.2	5.01 d (8.5)	121.5
6	0.52 t (3.0)	24.4	1.01	23.3	1.28	24.9
7	1.06	44.4	1.00	44.7	0.66 ddd (12.5, 9.0, 3.5)	27.0
8	α 1.43 m β 0.86 m	26.9	α 0.85 m β 1.45	27.7	α 1.67 β 0.91	19.3
9	α 0.58 dt (12.5, 2.0) β 1.66	31.8	α 1.65 β 0.54 ddd (15.0, 13.0, 2.0)	32.0	α 1.22 β 1.68	35.5
10	1.81 m	30.3	1.70	30.7	—	84.0
11	1.59	33.8	1.59	34.0	—	20.3
12	0.95 d (5.5)	20.1	0.96 d (6.5)	20.7	1.06 s	28.9
13	0.91 d (5.5)	20.0	1.02 d (6.5)	19.9	1.12 s	15.1
14	1.04 d (6.5)	19.1	0.96 d (7.0)	19.0	1.01 s	21.1
15	α 1.72 dd (14.0, 7.0) β 1.87 dd (14.0, 7.0)	29.4	α 1.70 β 1.72	30.0	1.71 s	17.2
1′	—	112.4	—	112.1	—	114.1
2′	—	198.2	—	198.0	—	197.8
3′	—	55.6	—	55.6	—	55.4
4′	—	213.9	—	213.9	—	214.0
5′	—	48.2	—	48.2	—	47.8
6′	—	170.7	—	172.3	—	170.0
7′	2.64 ddd (11.5, 7.0, 5.0)	34.5	2.75 td (9.0, 4.0)	33.6	2.61 dd (9.0, 2.0)	43.5
8′	2.56 m	26.9	2.60 m	26.5	2.08 m	30.9
9′	0.68 d (6.5)	16.3	0.64 d (6.5)	15.7	0.85 d (7.0)	19.7
10′	0.93 d (6.5)	20.8	0.96 d (6.5)	20.8	0.98 d (7.0)	20.4
11′	1.29 s	26.1	1.30 s	25.8	1.29 s	24.5
12′	1.40 s	24.5	1.40 s	24.6	1.32 s	24.3
13′	1.32 s	26.4	1.31 s	25.7	1.26 s	25.4
14′	1.32 s	23.1	1.31 s	23.5	1.34 s	24.3

[a] Data were recorded in $CDCl_3$ at 500 MHz for ^{1}H NMR and 125 MHz for ^{13}C NMR. [b] Overlapped signals are reported without designating multiplicity.

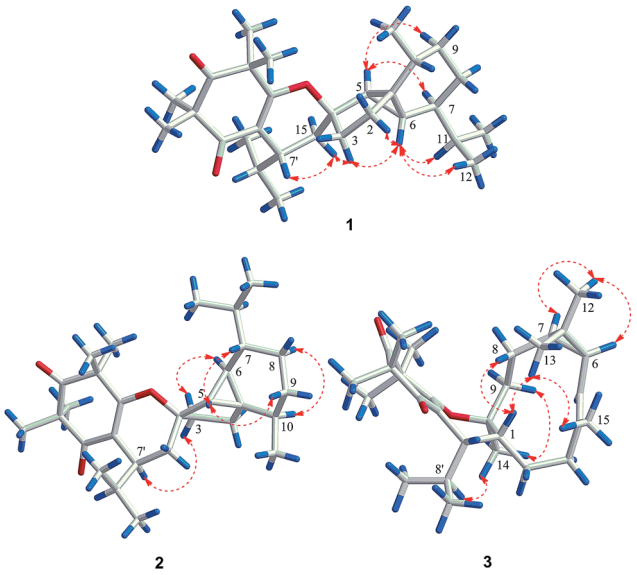

Fig. 3 Key NOESY correlations of **1**–**3**.

formula information as well as the upfield shift at C-6′ (δ_C 170.7) and downfield shift at C-4 (δ_C 90.5), the oxygen atom leftover was deduced to bridge C-4 and C-6′ to form a dihydropyran ring (Fig. 1).

In the NOESY spectrum, the correlations between H-5 and H-7/H-9α, between H-6 and H-2β/H-3β/H-11/Me-12, as well as between H-15β and H-3β/H-7′ established the relative configuration of **1** (Fig. 3). The complete structure and stereochemistry of **1** were further confirmed by an X-ray diffraction analysis. The final refinement of the Cu Kα data resulted in a small Flack parameter of −0.05 (11), allowing an unambiguous assignment of the absolute configurations of **1** as 1*R*, 4*S*, 5*R*, 6*R*, 7*S*, 10*R*, 7′*R* (Fig. 4).

Compound **2** gave the same molecular formula $C_{29}H_{44}O_3$ as **1** by its HR-ESI-MS data at *m*/*z* 441.3364 $[M + H]^+$ (calcd for $C_{29}H_{45}O_3$, 441.3363). Detailed examination of 1D and 2D NMR spectra of **2** and comparison with those of **1** revealed they have the same planar structure. Their different relative configurations were displayed by the different chemical shifts at C-4, C-7′, and H-7′ between **1** and **2**. The chiral centers of C-4 and C-7′ in **2** were established to have the opposite configurations to those of **1** through the NOESY correlations between H-5 and H-7/H-9β, between H-6 and H-3α, between H-10 and H-8α, as well as between H-7′ and H-3β (Fig. 3). The structure and relative configuration of **2** were further confirmed by X-ray crystallographic analysis (Fig. 4). To determine the absolute configurations of **2**, a comparison between the experimental and calculated circular dichroism (CD) spectra using the time-dependent DFT method was performed. The measured CD spectrum of **2** showed a positive Cotton effect at 304.5 ($\Delta\varepsilon$ +4.8) nm as well as a negative one at 260.7 ($\Delta\varepsilon$ −24.1) nm, which were consistent with those of the calculated CD spectrum for 1*R*, 4*R*, 5*R*, 6*R*, 7*S*, 10*R*, and 7′*S* isomer (Fig. 5). Hence, the absolute configurations of **2** were elucidated as 1*R*, 4*R*, 5*R*, 6*R*, 7*S*, 10*R*, and 7′*S*.

The molecular formula of **3** was determined to be $C_{29}H_{44}O_3$ by its HR-ESI-MS data at *m*/*z* 441.3370 $[M + H]^+$ (calcd for

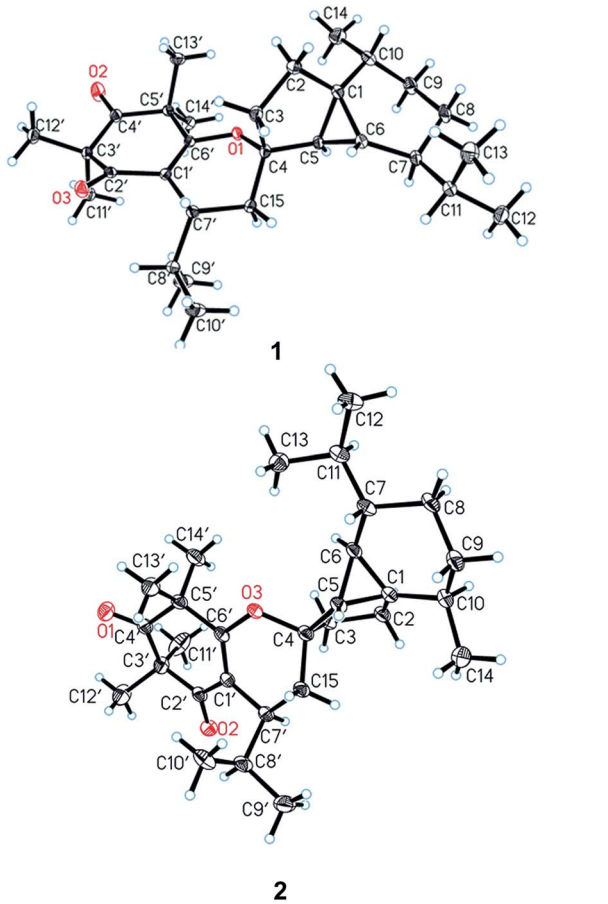

Fig. 4 X-ray ORTEP drawings of **1** and **2**.

$C_{29}H_{45}O_3$, 441.3363). Comparison of the NMR data of **3** with those of **1** and **2** (Table 1) suggested that they had the same substructure of an isobutyl syncarpic acid unit (a) (Fig. 2). The remaining 15 carbons was assigned to a sesquiterpene moiety. The ^1H–^1H COSY spectrum showed the presence of two spin systems (H-3 to H-9′/H-10′, and H-5 to H-9) (Fig. 2). Furthermore, the HMBC correlations between H-6/H-7/H-12/H-13 and C-11, between H-3 and C-4/C-5, between H-15 and C-4, between H-9 and C-1/C-10, as well as between H-14 and C-10 established the construction of a bicyclogermacrene unit (b) (Fig. 2). Moreover, the HMBC correlations between H-7′ and C-10/C-1′/C-2′/C-6′ indicated the connection of parts (a) and (b) *via* a C-1 and C-7′ bond. Finally, the closure mode of dihydropyran ring connecting the two fragments could be deduced on the basis of the molecular formula information as well as the upfield shift at C-6′ (δ_C 170.0) and downfield shift at C-10 (δ_C 84.0).

In the NOESY spectrum of **3**, the correlations between H-8β and H-1, between Me-13 and H-1/Me-15, between H-6/H-7 and Me-12, as well as between H-8′/H-9α and Me-14 confirmed the relative configurations of C-1, C-6, C-7, C-10, and C-7′ (Fig. 3). To determine the absolute configuration of **3**, the ECD curves for the two possible enantiomers (1*R*, 6*S*, 7*R*, 10*S*, 7′*S*-**3**, and 1*S*, 6*R*, 7*S*, 10*R*, 7′*R*-**3**) were respectively calculated using the time-dependent DFT method. The experimental CD spectrum of **3** exhibited positive Cotton effects at 294.2 ($\Delta\varepsilon$ +6.7) and 203.1 ($\Delta\varepsilon$

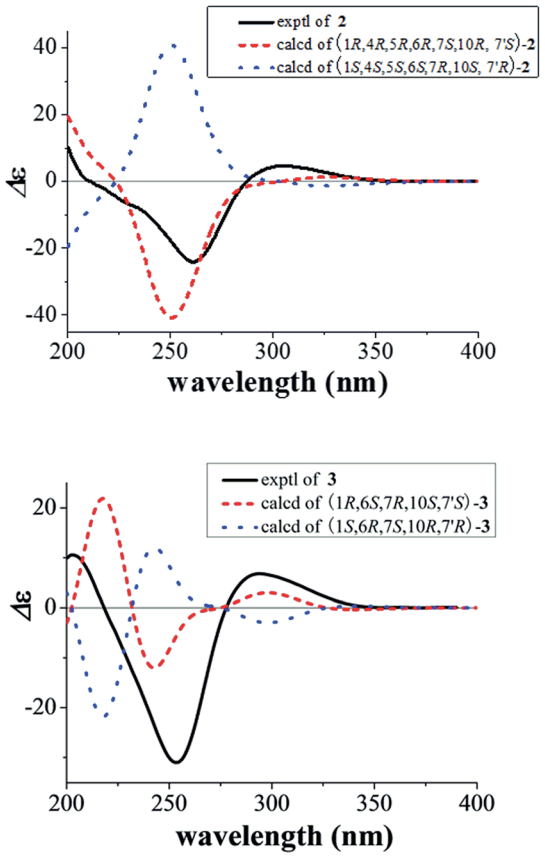

Fig. 5 Calculated and experimental CD spectra of **2** and **3**.

+10.5) nm as well as a negative one at 253.4 ($\Delta\varepsilon$ −31.0) nm, which were similar to the calculated curves of 1*R*, 6*S*, 7*R*, 10*S*, 7′*S*-**3** (Fig. 5). Thus, the structure of **3** was determined.

The known compounds callistiviminene J (**4**),[19] callistiviminene K (**5**),[19] callistiviminene M (**6**),[19] and callistiviminene N (**7**)[19] were identified by comparison of their physical and spectroscopic data with those reported in the literature.

The antiviral activities of phloroglucinol–terpene adducts from family Myrtaceae had been reported.[20,21] Thus, the antiviral effects of compounds **1–7** against respiratory syncytial virus (RSV) were evaluated in HEp-2 cells using the cytopathic effect (CPE) reduction assay. Compounds **3**, **5**, and **7** exhibited moderate inhibitory activities against RSV A2 strain with IC_{50} values ranging from 11.67 ± 0.95 to 15.85 ± 3.02 μM, while the IC_{50} value of the positive control ribavirin was 10.20 ± 0.90 μM. Cytotoxicity evaluation using the MTT (3-[4,5-dimethyl-thiazol-2-yl]-2,5-diphenyl tetrazolium bromide) assay showed that all compounds **1–7** were weak toxic to HEp-2 cells. Therefore, compound **5** showed the best antiviral selective induce (SI) (Table 2).

IC_{50} was detected by plaque reduction assay after the screening with CPE reduction assay; data are expressed as mean ± SD; CC_{50} was tested by MTT assay; data were expressed as mean ± SD; SI value equals to CC_{50}/IC_{50}.

In summary, three novel triketone–sesquiterpene adducts (**1–3**) along with four known ones (**4–7**) were isolated from the leaves of *Myrtus communis* 'Variegata'. Compounds **1** and **2** are a new type of meroterpenoids combined by β-triketone and cubebane units. The anti-RSV activities of compounds **1–7** are reported for the first time.

Table 2 *In vitro* anti-RSV A2 strain activities

Compounds	CC_{50} (μM)	IC_{50} (μM)	SI
1	>100	23.92 ± 1.46	>4.18
2	>100	31.04 ± 5.43	>3.22
3	77.87 ± 12.27	15.85 ± 3.02	4.91
4	>100	46.33 ± 3.75	>2.16
5	>100	11.67 ± 0.95	>8.57
6	95.55 ± 3.86	22.50 ± 2.50	4.25
7	58.03 ± 8.36	12.92 ± 1.91	4.49
Ribavirin	252.5 ± 6.8	10.20 ± 0.90	24.8

Experimental

General experimental procedures

Melting points were obtained on an X-5 micro melting point apparatus and are uncorrected (Fukai Instrument, Beijing, P. R. China). Optical rotations were measured on a JASCO P-2000 digital polarimeter (Jasco, Tokyo, Japan) at room temperature. UV spectra were determined on a JASCO V-550 UV/vis spectrophotometer (Jasco, Tokyo, Japan). IR spectra were recorded on a JASCO FT/IR-4600 plus Fourier transform infrared spectrometer (Jasco, Tokyo, Japan) using KBr pellets. ECD spectra were obtained on a JASCO J-810 spectropolarimeter (Jasco, Tokyo, Japan) at room temperature. HR-ESI-MS spectra were acquired on an Agilent 6210 LC/MSD TOF mass spectrometer (Agilent Technologies, CA, USA). NMR spectra were measured on Bruker AV-500 spectrometer (Bruker, Fällanden, Switzerland). Single-crystal data were performed using an Agilent Gemini S Ultra diffractometer and Cu Kα radiation. Silica gel (200–300 mesh; Qingdao Marine Chemical Inc., Qingdao, P. R. China), Sephadex LH-20 (Pharmacia Biotech AB, Uppsala, Sweden), and reversed-phase C_{18} silica gel (YMC, Kyoto, Japan) were used for column chromatography (CC). Preparative HPLC was carried out on an Agilent 1260 Chromatograph equipped with a G1311C pump and a G1315D photodiode array detector (Agilent Technologies, CA, USA) with a C_{18} reversed-phase column (Cosmosil, 10 × 250 mm, 5 μm). All solvents used in CC and HPLC were of analytical grade (Shanghai Chemical Plant, Shanghai, P. R. China) and chromatographic grade (Fisher Scientific, New Jersey, USA), respectively.

Plant material

The leaves of *M. communis* 'Variegata' were collected from Shanghai city of P. R. China in November 2015 and authenticated by Prof. Guang-Xiong Zhou, Jinan University, Guangzhou, P. R. China. A voucher specimen (no. 2015110701) was deposited in the Institute of Traditional Chinese Medicine and Natural Products, Jinan University, Guangzhou, P. R. China.

Extraction and isolation

The air-dried leaves of *M. communis* 'Variegata' (12 kg) were pulverized and extracted with 95% EtOH (V/V, 50 L) for 4 times at room temperature. The alcoholic extract was evaporated under

reduced pressure to give 2.1 kg crude extract, which was then suspended in water and extracted with petroleum ether (PE, b.p. 60–90 °C). The PE extract (412.5 g) was subjected to silica gel column chromatography eluted with a gradient mixture of cyclohexane/EtOAc (100 : 0 → 0 : 100) to afford twelve fractions (Fr. A–L). Fr. E (42.7 g) was separated by silica gel column chromatography with PE/EtOAc (100 : 0 → 0 : 100) as eluent to yield nine subfractions (Fr. E1–E9). Then, Fr. E3 (8.2 g) was subjected to ODS column chromatography using MeOH/H_2O (50 : 50 → 100 : 0) as eluent and further purified by reversed-phase semi-preparative HPLC (MeOH/H_2O, 90 : 10, 3 mL min^{-1}) to afford compounds **5** (14.5 mg, t_R 16.4 min), **1** (11.2 mg, t_R 35.8 min) and **2** (8.7 mg, t_R 38.7 min). Fr. E4 (2.3 g) was chromatographed on Sephadex LH-20 ($CHCl_3$/MeOH, 1 : 1) and purified by reversed-phase semi-preparative HPLC (MeOH/H_2O, 85 : 15, 3 mL min^{-1}) to obtain compounds **4** (6.2 mg, t_R 18.1 min) and **3** (10.3 mg, t_R 41.2 min). Fr. E5 (1.7 g) was also purified by reversed-phase semi-preparative HPLC (MeOH/H_2O, 80 : 20, 3 mL min^{-1}) to obtain compounds **6** (7.1 mg, t_R 18.7 min) and **7** (8.5 mg, t_R 20.5 min).

To confirm the purity of the samples for biological test, all compounds were analyzed by HPLC equipped with a diode array detector. The purities of compounds **1–7** calculated by area normalization method were between 96.22% and 99.99% (see ESI†).

X-ray crystallographic analysis of 1 and 2

The structure was solved by direct methods and refined by full-matrix least-squares on F^2 using SHELXL-97 package software. Crystallographic data for the structures have been deposited in the Cambridge Crystallographic Data Centre with the deposition number of CCDC 1529330 for **1** and CCDC 1529333 for **2** (see ESI†).

Crystal data of 1. $C_{29}H_{44}O_3$ (fw = 440.64); orthorhombic, space group $P2_12_12_1$; a = 6.0056(10) Å, b = 18.0532(4) Å, c = 23.3138(5) Å, $\alpha = 90°$, $\beta = 90°$, $\gamma = 90°$; V = 2527.69(9) $Å^3$, T = 293(2) K, Z = 4, D_c = 1.158 g cm^{-3}, $F(000)$ = 968. A total of 20 350 reflections were collected in the range $3.79 \leq \theta \leq 62.85$, of which 3815 unique reflections with $I > 2\sigma(I)$ were collected for the analysis. The final refinement gave R = 0.0299, R_w = 0.0779, S = 1.063 and Flack parameter = −0.05(11). Crystal data of **1** were deposited in the Cambridge Crystallographic Data Centre (CCDC 1529330).

Crystal data of 2. $C_{29}H_{44}O_3$ (fw = 440.64); triclinic, space group $P\bar{1}$; a = 9.7468(7) Å, b = 10.0413(9) Å, c = 14.7257(9) Å, α = 107.318(7)°, β = 95.676(6)°, γ = 104.090(7)°; V = 1311.43(18) $Å^3$, T = 100.01(10) K, Z = 2, D_c = 1.116 g cm^{-3}, $F(000)$ = 484. A total of 8553 reflections were collected in the range $4.76 \leq \theta \leq 73.61$, of which 3977 unique reflections with $I > 2\sigma(I)$ were collected for the analysis. The final refinement gave R = 0.0774, R_w = 0.2426, S = 1.032. Crystal data of **2** were deposited in the Cambridge Crystallographic Data Centre (CCDC 1529333).

Structure characterization

Myrtucomvalones A (1). Colorless blocks (MeOH); m.p. 182–183 °C; [α] = +52 (c 0.22, MeOH); UV (MeOH) λ_{max} (log ε): 204 (3.51), 268 (3.66) nm; IR (KBr) ν_{max}: 2957, 2925, 2854, 1714, 1651, 1620, 1466, 1381, 1333, 1171, 1154, 1038, 958, 896 cm^{-1}; HR-ESI-MS m/z 441.3369 $[M + H]^+$ (calcd for $C_{29}H_{45}O_3$: 441.3363); ^1H and ^{13}C NMR data, see Table 1.

Myrtucomvalones B (2). Colorless blocks (MeOH); m.p. 193–195 °C; [α] = +69 (c 0.24, MeOH); UV (MeOH) λ_{max} (log ε): 204 (3.58), 268 (3.78) nm; CD (CH_3CN) λ_{max} ($\Delta\varepsilon$): 211 (0), 261 (−24.1), 286 (0), 305 (+4.8) nm; IR (KBr) ν_{max}: 2924, 2851, 1717, 1654, 1612, 1464, 1381, 1316, 1170, 1134, 1039, 721 cm^{-1}; HR-ESI-MS m/z 441.3364 $[M + H]^+$ (calcd for $C_{29}H_{45}O_3$: 441.3363); ^1H and ^{13}C NMR data, see Table 1.

Myrtucomvalones C (3). Yellow oil; [α] = +116 (c 0.27, MeOH); UV (MeOH) λ_{max} (log ε): 210 (3.53), 267.5 (3.69) nm; CD (CH_3CN) λ_{max} ($\Delta\varepsilon$): 203 (+10.5), 218 (0), 253 (−31.0), 278 (0), 294 (+6.7) nm; IR (KBr) ν_{max}: 2975, 2871, 1716, 1651, 1622, 1459, 1383, 1178, 1117, 1050, 891 cm^{-1}; HR-ESI-MS m/z 441.3370 $[M + H]^+$ (calcd for $C_{29}H_{45}O_3$: 441.3363); ^1H and ^{13}C NMR data, see Table 1.

Cell and virus

Human larynx epidermoid carcinoma cells (HEp-2 cells, ATCC CCL-23) and human respiratory syncytial virus (RSV A2 strains, ATCC VR-1540) were obtained from Medicinal Virology Institute of Wuhan University in China. HEp-2 cells were grown in Dulbecco's modified eagle medium (DMEM, Gibco) containing 10% fetal bovine serum (FBS, Biological Industries) and 1% penicillin–streptomycin solution. The maintenance medium used for 3-(4,5-dimethyl-2-thiazolyl)-2,5-diphenyl tetrazolium bromide (MTT) and antiviral effect assay contained 2% FBS instead of 10%. Virus propagated on HEp-2 cells and were gathered when the lesion degree could be observed in the vast majority of cells. Viral titer expressed by 50% tissue culture infective dose ($TCID_{50}$) was tested by cytopathic effect (CPE) assay and the virus was stored at −80 °C.

Cytotoxicity assay

The cytotoxicity of compounds was estimated by MTT assay.[22] 1.5×10^4 cells per well were plated into 96-well plates and cultured at 37 °C in a 5% CO_2 incubator for 18 h. Then, growth medium was replaced by prepared compounds at concentrations of 3.125, 6.25, 12.5, 25, 50 or 100 μM in triplicate. After incubation for 48 h, the cells were treated with MTT solution for another 4 h. Subsequently, the supernatant was removed and dimethyl sulfoxide (DMSO) was added to dissolve the formazan. The absorbance was measured with a conventional microplate reader at 570 nm. Cell viability (%) was calculated as a percentage of absorbance of the medication administration team compared with the blank team. The 50% cytotoxic concentration (CC_{50}) was obtained by regression analysis of dose-response curves according to cell viability.

Antiviral effect assay

The antiviral effect of compounds was determined using a CPE reduction assay.[23] The antiviral activity of each compound was tested by using the maximal noncytotoxic concentration (MNCC) as the first concentration. Briefly, cell suspensions (1.5×10^4 cells per well) were seeded to each well in 96-well plates. After 18 h, monolayer of HEp-2 cells were treated with a mixture

of RSV (100 $TCID_{50}$) and different concentrations of compounds for 72 h. The development of CPE was monitored *via* formation of the syncytium. The antiviral effect of compounds could be manifested by observing the lesion degree of each well through microscope. The concentration inhibiting half of CPE was assessed from observations and was considered as the half maximal inhibitory concentration (IC_{50}).

Quantum chemical ECD calculation

The systematic random conformational analysis of compounds **2** and **3** were performed in Sybyl 8.1 program by using MMFF94 s molecular force field. All the obtained conformers were further optimized at B3LYP/6-31+G(d) level using the Gaussian 09 software.[24] The ECD calculation of each single conformer was carried out by means of time-dependent DFT (TDDFT) methods at the B3LYP/6-31+G(d) level, as available in Gaussian 09. The overall calculated ECD curves were obtained by means of Bolthzmann weighting of single ECD spectra. The calculated ECD spectra of **2** and **3** were subsequently compared with the experimental ones. The ECD spectra were produced by SpecDis 1.6 software.

Acknowledgements

This work was supported by Program for National Natural Science Foundation of China (No. U1401225, 81573307), the Science and Technology Planning Project of Guangdong Province (No. 2016B0-30301004), and the Guangdong Natural Science Foundation for Distinguished Young Scholar (No. 2015A030306022).

References

1 E. L. Ghisalberti, *Phytochemistry*, 1996, **41**, 7–21.
2 I. P. Singh and S. P. Bharate, *Nat. Prod. Rep.*, 2006, **23**, 558–591.
3 Z. C. Shang, M. H. Yang, K. L. Jian, X. B. Wang and L. Y. Kong, *Chem.–Eur. J.*, 2016, **22**, 11778–11784.
4 S. P. Yang, X. W. Zhang, J. Ai, L. S. Gan, J. B. Xu, Y. Wang, Z. S. Su, L. Wang, J. Ding, M. Y. Geng and J. M. Yue, *J. Med. Chem.*, 2012, **55**, 8183–8187.
5 Y. L. Zhang, C. Chen, X. B. Wang, L. Wu, M. H. Yang, J. Luo, C. Zhang, H. B. Sun, J. G. Luo and L. Y. Kong, *Org. Lett.*, 2016, **18**, 4068–4071.
6 R. W. Scora, *Phytochemistry*, 1973, **12**, 153–155.
7 O. Bazzali, F. Tomi, J. Casanova and A. Bighelli, *Flavour Fragrance J.*, 2012, **27**, 335–340.
8 M. Yoshimura, Y. Amakura, M. Tokuhara and T. Yoshida, *J. Nat. Med.*, 2008, **62**, 366–368.
9 M. I. Nassar, E. A. Aboutabl, R. F. Ahmed, E. A. El-Khrisy, K. M. Ibrahim and A. A. Sleem, *Pharmacogn. Res.*, 2010, **2**, 325–329.
10 F. Shaheen, M. Ahmad, S. N. Khan, S. S. Hussain, S. Anjum, B. Tashkhodjaev, K. Turgunov, M. N. Sultankhodzhaev, M. I. Choudhary and A. U. Rahman, *Eur. J. Org. Chem.*, 2006, **10**, 2371–2377.
11 C. Liu, S. Ang, X. J. Huang, H. Y. Tian, Y. Y. Deng, D. M. Zhang, Y. Wang, W. C. Ye and L. Wang, *Org. Lett.*, 2016, **18**, 4004–4007.
12 M. Shao, Y. Wang, Z. Liu, D. M. Zhang, H. H. Cao, R. W. Jiang, C. L. Fan, X. Q. Zhang, H. R. Chen, X. S. Yao and W. C. Ye, *Org. Lett.*, 2010, **12**, 5040–5043.
13 M. Shao, Y. Wang, Y. Q. Jian, X. J. Huang, D. M. Zhang, Q. F. Tang, R. W. Jiang, X. G. Sun, Z. P. Lv, X. Q. Zhang and W. C. Ye, *Org. Lett.*, 2012, **14**, 5262–5265.
14 Y. Q. Jian, Y. Wang, X. J. Huang, G. Q. Li, B. X. Zhao, Q. Y. Guo and W. C. Ye, *J. Asian Nat. Prod. Res.*, 2012, **14**, 831–837.
15 Y. Q. Jian, X. J. Huang, D. M. Zhang, R. W. Jiang, M. F. Chen, B. X. Zhao, Y. Wang and W. C. Ye, *Chem.–Eur. J.*, 2015, **21**, 9022–9027.
16 J. Q. Cao, X. J. Huang, Y. T. Li, Y. Wang, L. Wang, R. W. Jiang and W. C. Ye, *Org. Lett.*, 2016, **18**, 120–123.
17 B. P. S. Khambay, D. G. Beddie, A. M. Hooper, M. S. J. Simmonds and P. W. C. Green, *J. Nat. Prod.*, 1999, **62**, 1666–1667.
18 H. X. Liu, K. Chen, Y. Yuan, Z. F. Xu, H. B. Tan and S. X. Qiu, *Org. Biomol. Chem.*, 2016, **14**, 7354–7360.
19 L. Wu, X. B. Wang, R. J. Li, Y. L. Zhang, M. H. Yang, J. Luo and L. Y. Kong, *Phytochemistry*, 2016, **131**, 140–149.
20 M. Nishizawa, M. Emura, Y. Kan, H. Yamada, K. Ogawa and N. Hamanaka, *Tetrahedron Lett.*, 1992, **21**, 2983–2986.
21 V. Belekar, A. Shah and P. Garg, *Mol. Diversity*, 2013, **17**, 97–110.
22 L. Shi, H. Xiong, J. He, H. Deng, Q. Li, Q. Zhong, W. Hou, L. Cheng, H. Xiao and Z. Yang, *Arch. Virol.*, 2007, **152**, 1447–1455.
23 J. J. Xu, X. Wu, M. M. Li, G. Q. Li, Y. T. Yang, H. J. Luo, W. H. Huang, H. Y. Chung, W. C. Ye, G. C. Wang and Y. L. Li, *J. Agric. Food Chem.*, 2014, **62**, 2182–2189.
24 M. J. Frisch, G. W. Trucks, H. B. Schlegel, G. E. Scuseria, M. A. Robb, J. R. Cheeseman, G. Scalmani, V. Barone, B. Mennucci, G. A. Petersson, H. Nakatsuji, M. Caricato, X. Li, H. P. Hratchian, A. F. Izmaylov, J. Bloino, G. Zheng, J. L. Sonnenberg, M. Hada, M. Ehara, K. Toyota, R. Fukuda, J. Hasegawa, M. Ishida, T. Nakajima, Y. Honda, O. Kitao, H. Nakai, T. Vreven, J. A. Montgomery, Jr, J. E. Peralta, F. Ogliaro, M. Bearpark, J. J. Heyd, E. Brothers, K. N. Kudin, V. N. Staroverov, R. Kobayashi, J. Normand, K. Raghavachari, A. Rendell, J. C. Burant, S. S. Iyengar, J. Tomasi, M. Cossi, N. Rega, J. M. Millam, M. Klene, J. E. Knox, J. B. Cross, V. Bakken, C. Adamo, J. Jaramillo, R. Gomperts, R. E. Stratmann, O. Yazyev, A. J. Austin, R. Cammi, C. Pomelli, J. W. Ochterski, R. L. Martin, K. Morokuma, V. G. Zakrzewski, G. A. Voth, P. Salvador, J. J. Dannenberg, S. Dapprich, A. D. Daniels, O. Farkas, J. B. Foresman, J. V. Ortiz, J. Cioslowski, and D. J. Fox, *Gaussian 09, Revision B. 01*, Gaussian Inc., Wallingford, CT, 2010.

